

Emergence and dynamical properties of stochastic branching in the electronic flows of disordered Dirac solids

MARIOS MATTHEAKIS¹, G. P. TSIRONIS^{1,2} and EFTHIMIOS KAXIRAS^{1,3}

¹ *School of Engineering and Applied Sciences, Harvard University, Cambridge, Massachusetts 02138, USA*

² *Department of Physics, University of Crete, Heraklion 71003, Greece*

³ *Department of Physics, Harvard University, Cambridge, Massachusetts 02138, USA*

PACS 72.80.Vp – Electronic transport, graphene

PACS 05.10.Gg – Stochastic models in statistical physics and nonlinear dynamics

PACS 73.63.-b – Mesoscopic systems electronic transport

Abstract – Graphene as well as more generally Dirac solids constitute two dimensional materials where the electronic flow is ultra relativistic. When a Dirac solid is deposited on a different substrate surface with roughness, a local random potential develops through an inhomogeneous charge impurity distribution. This external potential affects profoundly the charge flow and induces a chaotic pattern of current branches that develops through focusing and defocusing effects produced by the randomness of the surface. An additional bias voltage may be used to tune the branching pattern of the charge carrier currents. We employ analytical and numerical techniques in order to investigate the onset and the statistical properties of carrier branches in Dirac solids. We find a specific scaling-type relationship that connects the physical scale for the occurrence of branches with the characteristic medium properties, such as disorder and bias field. We use numerics to test and verify the theoretical prediction as well as a perturbative approach that gives a clear indication of the regime of validity of the approach. This work is relevant to device applications and may be tested experimentally.

Introduction. – Wave focusing due to refractive index variation is a common occurrence in many physical systems. In sea waves, the effective refractive index variation arises from fluctuating depth [1–4]; in optical [5–10] or other media [11, 12] the index of refraction changes in a statistical way due to small imperfections or distributions of defects. Random spatial variability of the index leads to local focusing and defocusing of the waves and the formation of caustics or wave branches with substantially increased local wave intensity. Under general circumstances the branching flow develops a stochastic web with statistical patterns of persisting enhanced intensity wave motion. Since electrons have also wave properties due to their quantum nature, similar phenomena appear in the quantum realm. Injected electrons in disordered two dimensional (2D) electron gas form coalescing trajectories and manifest phenomena similar to wave motion in random media [13–16]. One aspect of the electronic motion that has not yet been explored is the relativistic and in particular the ultra-relativistic one; the latter occurs in materials referred to as Dirac solids (DS), such as graphene

[17–21]. In the ultra-relativistic limit, the magnitude of the Dirac fermion velocity cannot be affected by external fields as it is already at its maximum value, leading to significant differences from the conventional non-relativistic flow. This is directly reflected in the electronic branching properties and gives rise to discernible differences, as we show here.

Pristine graphene is the prototypical 2D-DS, characterized by linear dispersion in the electronic band structure near the Fermi level [17, 18],

$$\epsilon_{\mathbf{k}} = v_F \hbar |\mathbf{k}|, \quad (1)$$

where $\epsilon_{\mathbf{k}}$ is the single particle energy, v_F is the Fermi velocity and \mathbf{k} is the wave-vector. Electron flow in these band segments is ultra-relativistic with maximal propagation velocity v_F [17, 21–24]. This electron flow is modified by the presence of a bias potential applied along a specific direction. The relativistic electronic dispersion couples the motion of electrons along the direction of bias and the one perpendicular to it [22, 23]. Electron dynamics is also subject to the presence of substitutional or other type

of weak disorder; the effects of such disorder are observed in graphene in the form of electronic puddles [24–28]. The combined presence of disorder and bias alters the electronic flow and thus the ultra-relativistic trajectories coalesce into branches of substantial local density. In this letter we show that the weak surface disorder produces a lensing mechanism for the electronic waves that is clearly manifested in the form of caustics. Dirac fermions cannot be accelerated by a bias potential, in contrast to the corresponding behavior of non-relativistic electrons in 2D metals with parabolic bands. As a result, a simple relationship derived here between the caustic location and statistical properties of the intrinsic potential remains valid even in the presence of external fields; we derive this scaling-type formula analytically and verify it by numerical simulations. Scanning probe microscope (STM) techniques have been used extensively to measure the electron density [20] and in turn, the branching flow in 2D electron gases [13, 15].

Theoretical Analysis. – The basic feature of a 2D-DS is the linear dispersion relation of the energy with wave-vector, Eq. (1). When the electronic density is low we may use the independent electron model to describe the quasi-classical dynamics of charge carriers [22, 23] through the quasi-classical ultra-relativistic Hamiltonian

$$\mathcal{H} = \pm v_F \sqrt{p_x^2 + p_y^2} + V(x, y), \quad (2)$$

where $\mathbf{p} = (p_x, p_y)$ is the 2D momentum of the charge carriers. The Hamiltonian (2) is the classical limit of Dirac equation [22] that describes dynamics of massless electron/hole quasi-particles in graphene and other DS [18]. Branched flow is an effect of ray fields associated with waves [1, 4, 11] and thus, we may use the Hamiltonian (2) to give a ray description of the quantum flow of Dirac electrons. We note that STM measurements have shown that classical ray-tracing simulations describe accurately the electron flow in graphene [20].

We focus on 2D ultra-relativistic dynamics of particles in a medium with potential $V(x, y) = V_r(x, y) + V_d(x)$, where $V_r(x, y)$ is a random δ -correlated potential with energy scale much smaller than that of the electronic flow; this term comes from random charged impurities in the substrate or other sources of disorder in the graphene sheet [24–28]. The deterministic “control” potential $V_d(x) = -\alpha x$ is due to an externally applied voltage in the x -direction with α fixed by experimental conditions. Electrons are injected in the Dirac sheet with initial momentum p_0 along the x -direction; due to the ballistic electronic motion along the x -axis we may ignore the effects of the random potential in this direction [14, 16]. We use plane wave initial conditions for the electrons, $p_x(0) = p_0$ and $p_y(0) = 0$, and write the corresponding solution of Hamilton’s equations as $p_x(t) = p_0 + \alpha t$ and $p_y(t) = -\int \partial_y V_r(x, y) dt$, with $p_x \gg p_y$. We expand the Hamiltonian (2) up to second order in p_y/p_x to obtain

$$\mathcal{H} = p_x + \frac{p_y^2}{2p_x} + V(x, y), \quad (3)$$

and set $v_F = p_0 = 1$ for simplicity. In order to study wave-like electronic flow through the Hamilton-Jacobi equation (HJE) we introduce the classical action S with $p_x = \partial_x S$ and $p_y = \partial_y S$, and express the HJE as

$$\partial_t S + \partial_x S + \frac{(\partial_y S)^2}{2\partial_x S} + V(x, y) = 0. \quad (4)$$

Employing previous non-relativistic approaches to the branching problem we derive an equation for the local curvature of the electronic flow determined through $u = \partial_{yy} S$ [5, 8]. To this effect we apply the operator $\hat{T} \equiv (\partial_{xx} + \partial_{yy} + 2\partial_{xy})$ on Eq. (30) and obtain

$$\partial_t u + \frac{u^2}{\partial_x S} + \frac{\partial_y S}{\partial_x S} \partial_y u + \hat{T} V(x, y) = 0. \quad (5)$$

Using the effective Hamiltonian (3) we calculate the equations of motion for the x , p_x conjugate variables keeping the lowest order terms in p_y/p_x , which leads to the simple relation $x(t) = t$. Thus, under the approximation of the dominance of the momentum in the forward x -direction, we find that space and time variables are identical. We use this fact to simplify the HJE ray dynamics and turn Eq. (5) into a quasi-2D version [1, 5], that is, we replace the space coordinate x with t and use $\hat{T} V = \partial_{yy} V_r(t, y)$; this simplification is valid only in the ultra-relativistic limit since non-relativistic electrons accelerate in the presence of non-zero values for the parameter α .

We need to calculate the convectional derivative for u ; for an arbitrary function $f(\mathcal{H})$, where \mathcal{H} is the Hamiltonian (3) we have

$$\frac{df}{dt} = \left[\partial_t + \frac{\partial x}{\partial t} \partial_x + \frac{\partial y}{\partial t} \partial_y \right] f. \quad (6)$$

In quasi-2D approximation the potential depends only on time and transverse coordinate y , i.e. $V \equiv V(t, y)$; subsequently, the term that includes the operator ∂_x is zero. On the other hand, the term $\partial y/\partial t$ can be determined by Hamilton’s equations of (3) as

$$\frac{\partial y}{\partial t} = \frac{dy}{dt} = \frac{\partial \mathcal{H}}{\partial p_y} = \frac{p_y}{p_x} \quad (7)$$

Using the definition of the classical action S , namely $p_x = \partial_x S$ and $p_y = \partial_y S$, and the Eqs. (6) and (7) we obtain the convectional derivative formula:

$$\frac{df}{dt} = \left[\partial_t + \frac{\partial_y S}{\partial_x S} \partial_y \right] f. \quad (8)$$

Using the expression of Eq. (8) for the convectional derivative in conjunction with the approximate quasi-one dimensional Hamiltonian of Eq. (3) we obtain an ordinary non-linear differential equation for the local wave curvature:

$$\frac{du}{dt} + \frac{u^2}{1 + \alpha t} + \partial_{yy} V_r(t, y) = 0. \quad (9)$$

The dynamics of Eq. (9) determines the onset of the regime for caustics; this occurs at times, or equivalently locations along the x -axis, where the curvature u becomes singular [5, 14, 16]. The first time when a singularity in u occurs determines the precise point for the onset of ray coalescence. Given that the term $\partial_{yy} V_r(t, y)$ is fluctuating, we solve the first passage time problem for the curvature to reach $|u(t_c)| \rightarrow \infty$, where t_c is the time for the occurrence of the first caustic.

Deterministic caustic dynamics. – We may obtain a useful and intuitive expression for the onset of branches if we ignore at first the stochastic potential term of Eq. (9); straightforward solution of the resulting simple nonlinear equation leads to the solution

$$t_c = \frac{e^{\alpha/|u_0|} - 1}{\alpha}, \quad (10)$$

where we set $u_0 = -|u_0|$ since negative initial curvature leads to positive t_c . In the strong external potential limit ($\alpha \rightarrow \infty$) the caustic needs infinite time to develop ($t_c \rightarrow \infty$), while in the weak limit of ($\alpha \rightarrow 0$) t_c is finite and increases linearly with α ,

$$t_c = \frac{1}{|u_0|} \left(1 + \frac{\alpha}{2|u_0|} \right). \quad (11)$$

This behavior follows from the effective elimination of the nonlinear term in u of Eq. (9), in the large α limit, which is responsible for the creation of caustic events.

Along the propagation axis t , the fluctuating term in Eq. (9) acts as a δ -correlated noise $\xi(t)$ with zero mean and standard deviation σ , $\partial_{yy} V_r(t, y) = \sigma^2 \xi(t)$, and Eq. (9) becomes a stochastic Langevin equation [4, 14, 16]. For $\alpha = 0$ the curvature Eq. (9) reduces to the non-relativistic case with the average first caustic time $\langle t_c \rangle$ obeying the scaling relationship $\langle t_c \rangle \sim \sigma^{-2/3}$ [1, 5, 16].

Self-consistent equation for the onset of branches. – To quantify the location of the occurrence of the first relativistic caustic event including α , we use a self-consistent approach. Specifically, we start from the more general equation

$$\frac{du}{dt} = -\frac{u^2}{p_0 + \alpha(t - t_0)} - \sigma^2 \xi(t), \quad (12)$$

where α is the deterministic control parameter, σ is the standard deviation of random potential, and ξ a white noise with unit variance. To find self-consistently a new scaling-type relationship we assume $t = \langle t_c \rangle$ turning Eq. (12) to

$$\frac{du}{dt} = -\gamma u^2 - \sigma^2 \xi(t), \quad (13)$$

where γ is a constant defined as

$$\gamma = \frac{1}{p_0 - \alpha t_0 + \alpha \langle t_c \rangle}. \quad (14)$$

The Eq. (13) has been treated in refs. [5, 8] for the simpler case of $\gamma = 1$ yielding $\langle t_c \rangle = 3.32\sigma^{-2/3}$. Following the same stochastic approach for $\gamma \neq 1$, we obtain the more general formula

$$\langle t_c \rangle = 3.32(\sigma\gamma)^{-2/3}. \quad (15)$$

The new expression is derived after the solution of the self-consistent set of Eqs. (14) and (15); the combined equation is given by

$$Ax^3 + Bx^2 + 1 = 0 \quad (16)$$

where

$$A = -\frac{3.32^{-3/2}}{p_0 - \alpha t_0} \sigma, \quad B = \frac{\alpha}{p_0 - \alpha t_0}, \quad x = \langle t_c \rangle^{1/2}. \quad (17)$$

The only real solution of the Eq. (16) is

$$x = \frac{B}{3A} \left(1 + \frac{B}{c} + \frac{c}{B} \right), \quad (18)$$

where

$$c = \left[\frac{27A^2}{2} \left(1 + \frac{2B^3}{27A^2} + \sqrt{1 + \frac{4B^3}{27A^2}} \right) \right]^{1/3}. \quad (19)$$

Since α and σ are assumed to have small values, we define the small coefficient

$$\tilde{\alpha} = \frac{BA^{-2/3}}{3} \ll 1. \quad (20)$$

Substitution of Eq. (20) in (19) and expanding for small $\tilde{\alpha}$ yields approximately to

$$c = 3A^{2/3} \left(1 + \frac{2}{3}\tilde{\alpha}^3 \right). \quad (21)$$

We use Eq. (21) in (18) and expand up to $\tilde{\alpha}^3$ to obtain

$$x = -A^{-1/3} \left(1 + \tilde{\alpha} + \tilde{\alpha}^2 + \frac{2}{3}\tilde{\alpha}^3 \right). \quad (22)$$

Using Eqs. (17) and (22), we find the ultra-relativistic formula for the first caustic time

$$\langle t_c \rangle = 3.32 \left(\frac{\sigma}{p_0 - \alpha t_0} \right)^{-2/3} \left(1 + 2\tilde{\alpha} + 3\tilde{\alpha}^2 + \frac{10}{3}\tilde{\alpha}^3 \right) \quad (23)$$

with

$$\tilde{\alpha} = 1.11 \frac{\alpha \sigma^{-2/3}}{(p_0 - \alpha t_0)^{1/3}}. \quad (24)$$

Choosing a more convenient set of initial values, i.e. $t_0 = 0$ and $p_0 = 1$, yields to

$$\langle t_c \rangle \sim \sigma^{-2/3} \left(1 + 2\tilde{\alpha} + 3\tilde{\alpha}^2 + \frac{10}{3}\tilde{\alpha}^3 \right), \quad (25)$$

with $\tilde{\alpha} = 1.11\alpha\sigma^{-2/3}$ the relativistic correction term in the presence of a deterministic potential. We note that for $\tilde{\alpha} = 0$ we obtain the previously obtained expression for not relativistic branches [16].

Numerical solution of the Hamilton-Jacobi Equation. – We now depart from the quasi-2D approximation and solve numerically the characteristic equations for the full Hamiltonian (2) while constructing a random potential based on experimental observations. In particular, impurities in the substrate of graphene create a smooth landscape of charged puddles of radius $R \approx 4$ nm [27, 28]. In our model, each puddle size is drawn from a two-dimensional Gaussian distribution with standard deviation R . The location of each puddle is randomly chosen through a uniform distribution. We perform simulations for quasi-classical electron dynamics in a graphene sheet of size 400×400 nm, where several caustics are observed; periodic boundary conditions are used to ensure that all the rays reach a caustic. The random potential consists of 2000 randomly distributed Gaussian defects with $R = 4$ nm. A collection of 1000 ultra-relativistic rays, initially distributed uniformly along y axis, are injected into the graphene sheet from the $x = 0$, with plane wave initial conditions, $p_x(0) = p_0 = 1$ and $p_y(0) = 0$. We select a single caustic event out of many to show how the deterministic part of the potential affects the onset of this event, see Fig. 1. The rays propagate in the disordered potential with $\sigma = 0.1$ and after time t_c a caustic event occurs. The ray-tracing simulations are performed for three different values of $\alpha = [0, 0.05, 0.1]$, to show that t_c increases linearly with α , a behavior expected from Eq. (11). We thus confirm numerically the quasi-2D analytical prediction that the presence of a small voltage in graphene shifts the location of the first caustic, a fact that can be tested experimentally. The location and the shape of caustics are modified by the external potential V_d ; in particular, as α increases the passage to branched flow is delayed and the caustics disperse slower, see Fig. 1.

Phase space approach. – The classical electron trajectories can be used to determine the onset of a caustic in the context of the stability matrix \mathcal{M} . The latter describes the evolution in time of an infinitesimal volume of phase space, $\delta x_i(t) = \mathcal{M} \delta x_i(0)$, where $x_i = (x, y, p_x, p_y)$ is the four dimensional phase space vector, and the elements of \mathcal{M} read $m_{ij}(t) = \partial x_i(t) / \partial x_j(0)$ [12, 16]. The evolution of \mathcal{M} is given by $\dot{\mathcal{M}}(t) = \mathbf{K} \mathcal{M}(t)$ with initial condition $m_{ij}(0) = \delta_{ij}$, i.e.

$$\dot{\mathcal{M}}(t) = \begin{pmatrix} 0 & \mathbb{1} \\ -\mathbb{1} & 0 \end{pmatrix} \frac{\partial^2 \mathcal{H}}{\partial x_i \partial x_j} \mathcal{M}(t) = \mathbf{K} \mathcal{M}(t), \quad (26)$$

where $\mathbb{1}$ is the identity matrix. For Dirac fermions the symplectic matrix \mathbf{K} is obtained from the ultra-relativistic Hamiltonian:

$$\mathbf{K} = \begin{pmatrix} 0 & 0 & p_y^2/p^3 & -p_x p_y/p^3 \\ 0 & 0 & -p_x p_y/p^3 & p_x^2/p^3 \\ -V_{xx} & -V_{xy} & 0 & 0 \\ -V_{xy} & -V_{yy} & 0 & 0 \end{pmatrix}, \quad (27)$$

where $p = |\mathbf{p}| = \sqrt{p_x^2 + p_y^2}$. A caustic occurs when the classical density of rays diverges giving rise to the con-

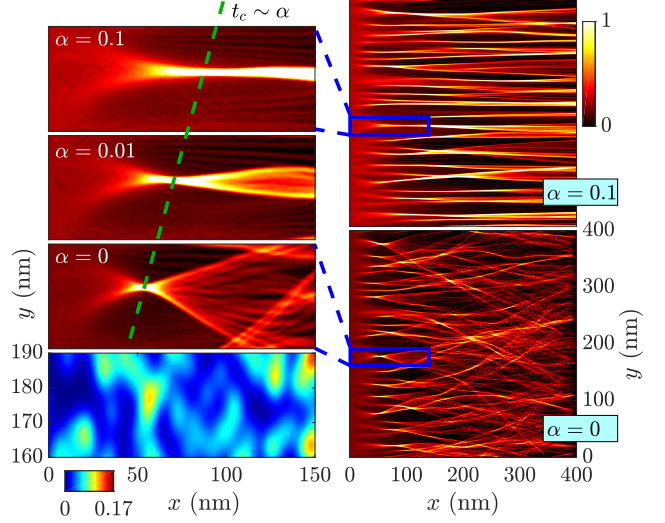


Fig. 1: Two-dimensional numerical ray-simulations determine the onset of a caustic event in a disordered potential with $\sigma = 0.1$ and for a deterministic potential with $\alpha = [0, 0.05, 0.1]$. (Left) The lower panel shows the random potential. The remaining images represent the density of rays I . The green dashed line shows that the first caustic time t_c increases linearly with α . (Right) The ray density of branched flow in a graphene sheet for $\alpha = 0$ and $\alpha = 0.1$.

dition for caustic emergence $(-p_y, p_x, 0, 0)^T \mathcal{M} \delta x_i(0) = 0$ [12]. We use this condition to determine numerically the time t_c where the first caustic occurs by calculating the average time needed for the first caustic event. To this end we study a wide range of strength for the Gaussian defects in order to obtain many V_r with different variances σ^2 . In addition, we examine several bias potentials with α ranging between 0 and 0.1 while realizing 30 disorder potentials for each pair of σ and α values. Furthermore, in these simulations we consider 10^4 ultra-relativistic electrons distributed uniformly along y and ejected at $x = 0$. In Fig. 2 we present the relation between $\langle t_c \rangle$ and the potential parameters (σ, α) . For $\alpha = 0$ we obtain $\langle t_c \rangle \sim \sigma^{-2/3}$, the scaling of conventional 2D metals in the absence of bias potential [14, 16]. When $\alpha \neq 0$, $\ln(\langle t_c \rangle)$ decays practically linearly with $\ln(\sigma)$ revealing that the ultra-relativistic nature of Dirac fermions retains the scaling also in the presence of a bias potential, as predicted theoretically by Eq. (25). The color solid lines show the theoretical prediction of $\langle t_c \rangle$ through the use of Eq. (25) in the range that is valid, $\alpha \sigma^{-2/3} \ll 1$.

Dirac solids with a gap. – The spatiotemporal trajectories may be altered when structural defects are present in graphene. In this case a small energy gap appears in the electronic band structure, which leads to a discernible electronic effective mass m [18, 19]. In this case the free carriers are described by the relativistic Hamiltonian [22]

$$\mathcal{H} = \pm v_F \sqrt{p_x^2 + p_y^2 + m^2} + V(x, y). \quad (28)$$

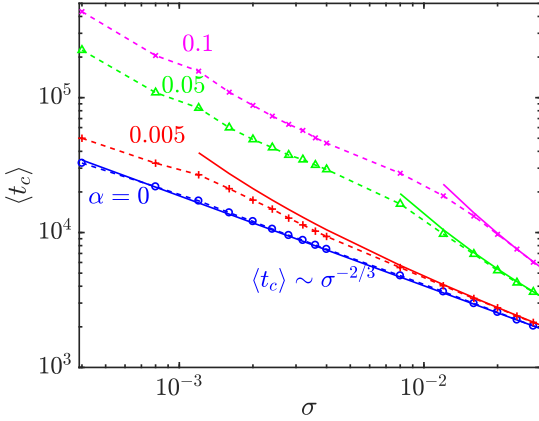


Fig. 2: Simulation results for the mean first caustic time $\langle t_c \rangle$ for the occurrence of a caustic event as a function of the random potential standard deviation σ and for bias determined by α in the range $[0, 0.1]$ (dashed lines connect data points). The color solid lines indicate the theoretical predicted relationship between $\langle t_c \rangle$ and σ in log space, in the range where Eq. (25) is valid.

When electrons move very fast in x direction ($p_x \gg p_y$) and the effective mass is very small ($p_x \gg m$), we expand the Hamiltonian (28) up to second order of m/p_x and p_y/p_x to obtain

$$\mathcal{H} = p_x + \frac{p_y^2 + m^2}{2p_x} + V(x, y), \quad (29)$$

where for convenience we set $v_F = 1$. The Hamilton-Jacobi equation of Eq. (29) reads

$$\partial_t S + \partial_x S + \frac{(\partial_y S)^2 + m^2}{2\partial_x S} + V(x, y) = 0. \quad (30)$$

where the classical action S is defined as $p_x = \partial_x S$ and $p_y = \partial_y S$. In turn, we follow the same methodology that discussed in the main text to calculate an approximate equation for the local curvature of the electronic flow determined through $u = \partial_{yy} S$:

$$\frac{du}{dt} + \frac{u^2}{p_0 + \alpha t} + \partial_{yy} V_r(t, y) = 0. \quad (31)$$

We observe that the curvature equation (31) is independent of m and thus, the Dirac branched electronic flow dynamics is not affected by small defects in Dirac solids. We infer that Dirac branching is robust and not affected by the presence of few structural defects in graphene.

Conclusions. — Branching is a stochastic, spatiotemporal phenomenon that relates to the self-organization of flows in extended complex systems ranging from geophysics, to optics, to materials science and beyond. The necessary condition for the occurrence of stochastic branching is the presence of wave-like motion in a typically weakly random environment. The latter acts as a

random index of refraction in the propagation of waves and, as a result, non-deterministic focusing and defocusing events generate wave coalescence. The onset of branches are seen as singularities of the wave-fronts, i.e. caustics, and as such may be investigated analytically via effectively stochastic differential equations. Previous work has shown that the onset and location of branching events in electronic systems scales with the statistical properties of the medium [16]. These results are important both from the theoretical but also in practice since the onset of charge singularities is not desirable in actual devices.

The unifying theme in the onset of branching is the existence of wave motion in a random medium. While in geophysical or optical systems wave motion is clear, to have wave motion in materials we need to invoke wave properties of electrons or other carriers. Electrons, as quantum particles, do have wave properties; however what is needed for branching is the collective propagation of the electrons in an organized or spatiotemporally complex flow. This flow is induced by the collective ensemble of the electrons as they propagate in the random medium. As has been shown clearly previously [16], this dynamics is adequately described as a classical, non-relativistic, phase space flow. Thus, we may conclude that branching phenomena in materials are complex phenomena induced in a corpuscular ensemble through spatial disorder and involve macroscopic focusing and singularities.

In the present work we departed from the previous analyses in material systems and focused uniquely on two dimensional novel materials such as graphene and more generally Dirac solids. As is well known, the electronic dispersion relation in these systems is fundamentally linear (and not quadratic, as is typically in most conventional materials) leading to effective relativistic and more specifically ultra-relativistic carrier motion. Following an approach compatible with other works in these systems [22] we analyzed the ultra-relativistic Hamilton-Jacobi flow problem using both analytics and exact numerics and found that also in these relativistic flows branching persists. In particular the ultra-relativistic caustic events occur as a result of the random particle propagation in the two dimensional random potential and that increasing the external bias, shifts the onset of the branches to latter lattice locations. We derived a specific equation that connects the location of these events to the statistical properties of the medium as well as the bias strength. This expression, that reduces to the previously derived law for the non-relativistic motion in the appropriate limit [16] has been fully verified computationally. A remarkable finding is that the bias field may tune the branching location and thus the phenomenon may be tested directly experimentally. The phenomena described and predicted in this work are related to known charge puddles in graphene [24–28] and future experimental but also theoretical work in two dimensional Dirac solids should point in this direction.

* * *

We acknowledge support by ARO MURI Award No. W911NF-14-0247 (M.M., E.K.), EFRI 2-DARE NSF Grant No. 1542807 (M.M.), European Union project NHQWAVE MSCA-RISE 691209 (G.P.T.). We used computational resources on the Odyssey cluster of the FAS Research Computing Group at Harvard University. M.M. and G.P.T. acknowledge helpful discussions with Dr. Ragnar Fleischmann and Dr. Jakob J. Metzger.

REFERENCES

- [1] DEGUELDRE H., METZGER J. J., GEISEL T. and FLEISCHMANN R., *Nature Physics*, **12** (2016) 259.
- [2] HELLER E., *Nature Physics*, **12** (2016) 824.
- [3] COUSINS W. and SAPSIS T. P., *Journal of Fluid Mechanics*, **790** (2016) 368-388.
- [4] DEGUELDRE H., METZGER J. J., SCHULTHEIS E. and FLEISCHMANN R., *Phys. Rev. Lett.*, **118** (2017) 024301.
- [5] KLYATSKIN V. I., *Waves in Random Media*, **3** (1993) 93-100.
- [6] NI X., LAI Y. C. and WANG W. X., *Chaos*, **22** (2012) 043116.
- [7] BARKHOFEN S., METZGER J. J. FLEISCHMANN R. KUHL U. and STÖCKMANN H. J., *Phys. Rev. Lett.*, **111** (2013) 183902.
- [8] MATTHEAKIS M. and TSIRONIS G. P., *Quodons in Mica*, edited by ARCHILLA J., JIMÉNEZ, N., SÁNCHEZ-MORCILLO V. and GARCÍA-RAFFI L. 2015, Vol. **221** (Springer), p. 425-454
- [9] MATTHEAKIS M., PITSIOS I. J., TSIRONIS G. P. and TZORTZAKIS S., *Chaos, Solitons and Fractals*, **84** (2016) 73-80.
- [10] SAFARI A., FICKLER R., PADGETT M. J. and BOYD R. W., *Phys. Rev. Lett.*, **119** (2017) 203901.
- [11] WOLFSON M. A. and TAPPERT F. D., *The Journal of the Acoustical Society of America*, **107** (2000) 154-162.
- [12] WOLFSON M. A. and TOMSOVIC S., *The Journal of the Acoustical Society of America*, **109** (2001) 2693-2703.
- [13] TOPINKA M. A., LEROY B. J., WESTERVELT R. M., SHAW S. E. J., FLEISCHMANN R., HELLER E. J., MARANOWSKI K. D., and GOSSARD A. C., *Nature*, **410** (2001) 183-186.
- [14] KAPLAN, L., *Phys. Rev. Lett.*, **89** (2002) 184103.
- [15] JURA M. P., TOPINKA M. A., URBAN L., YAZDANI A., SHTRIKMAN, H., PFEIFFER L. N., WEST K. W. and GOLDHABER-GORDON D., *Nature Physics*, **3** (2007) 2007.
- [16] METZGER J. J., FLEISCHMANN R., and GEISEL T., *Phys. Rev. Lett.*, **105** (2010) 020601.
- [17] NOVOSELOV K. S., GEIM A. K., MOROZOV S. V., JIANG D., KATSNELSON M. I., GRIGORIEVA I. V., DUBONOS S. V., and FIRSOV A. A., *Nature*, **438** (2005) 197-200.
- [18] WEHLING T.O., BLACK-SCHAFFER A.M., and BALATSKY A.V., *Advances in Physics*, **63** (2014) 1-76.
- [19] KUMAR A., NEMILENTSAU A., FUNG K. H., HANSON G. F., NICHOLAS X. and LOW T., *Phys. Rev. B*, **93** (2016) 041413.
- [20] BHANDARI S., LEE G. H., KLALES A., WATANABE K., TANIGUCHI T., HELLER E., KIM P., and WESTERVELT R. M., *Nano Letters*, **16** (2016) 1690-1694.
- [21] CROSSNO J. *et al.*, *Science*, **351** (2016) 1059-1061.
- [22] POTOTSKY A., MARCHESONI F., KUSMARTSEV F. V. HÄNGGI P. and SAVELEV S. E., *The European Physical Journal B*, **85** (2012) 356.
- [23] POTOTSKY A. and MARCHESONI F., *Phys. Rev. E*, **87** (2013) 032132.
- [24] MARTIN J., AKERMAN N., ULBRICHT G., LOHMANN T., SMET J. H., VON KLITZING K., and YACOBY, A., *Nature Physics*, **4** (2008) 144.
- [25] TAN Y. W., ZHANG Y., BOLOTIN K., ZHAO Y., ADAM S., HWANG E. H., DAS SARMA S., STORMER H. L. and KIM P., *Phys. Rev. Lett.*, **99** (2007) 246803.
- [26] ZHANG Y., BRAR V. W., GIRIT C., ZETTL A. and CROMMIE M. F., *Nature Physics*, **5** (2009) 722.
- [27] MARTIN S. C., SAMADDAR S., SACÉPÉ B., KIMOUCHE A., CORAUX J., FUCHS F., GRÉVIN B., COURTOIS H. and WINKELMANN C. B., *Phys. Rev. B*, **91** (2015) 041406.
- [28] SAMADDAR S., YUDHISTIRA I., ADAM S., COURTOIS H. and WINKELMANN C. B., *Phys. Rev. Lett.*, **116** (2016) 126804.